Supporting Information

Patterned Electrode-Based Amperometric Gas Sensor for Direct Nitric Oxide Detection within Microfluidic Devices

Wansik Cha, Yi-Chung Tung, Mark E. Meyerhoff[#] and Shuichi Takayama[*]

Department of Bioengineering, University of Michigan, 2200 Bonisteel Blvd., Ann Arbor, Michigan 48109-2099

and

[#]Department of Chemistry, University of Michigan, 930 N. University Ave., Ann Arbor, MI 48109-1055

(a)

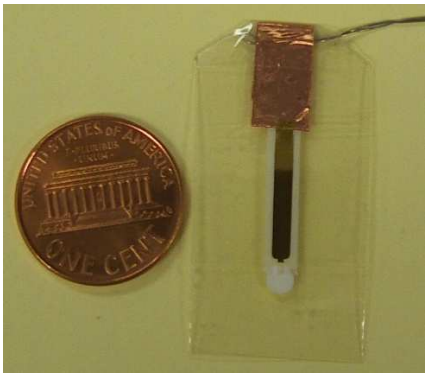

(b)

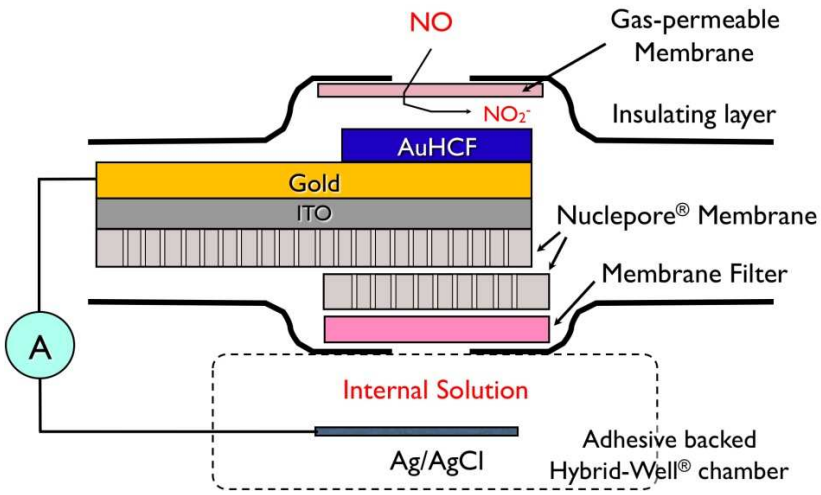

Figure S1. (a) Image of WE half-cell assembly, front side. Overall thickness is ~ 300 µm. (b) Schematic diagram of cross section of novel NO sensor proposed in this work. TeflonAF®-treated Celgard® membrane is used as gas-permeable membrane.

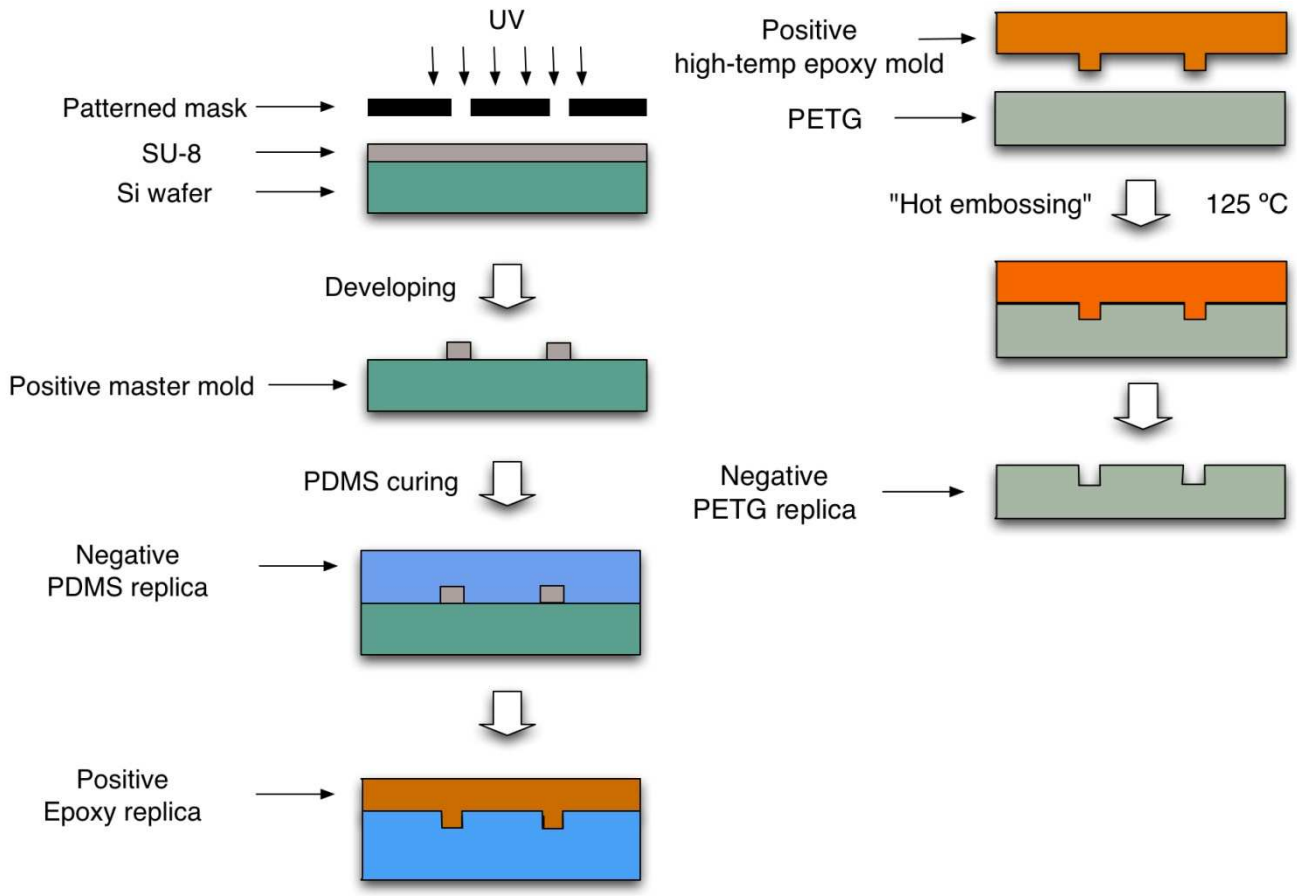

Figure S2. Schematic representation of microfluidic device fabrication procedure. (a) Procedure for positive replica of high-temperature epoxy mold. Soft-lithography method was used in initial processes. Two-component high temperature epoxy (Cytec FR1080) was cured at 80 ºC overnight on negative replica of PDMS mold. (b) Hot-embossing procedure to obtain negative PETG replica. Cured epoxy mold can be used many times for production of PETG devices via hot-press procedure at 125 ºC.

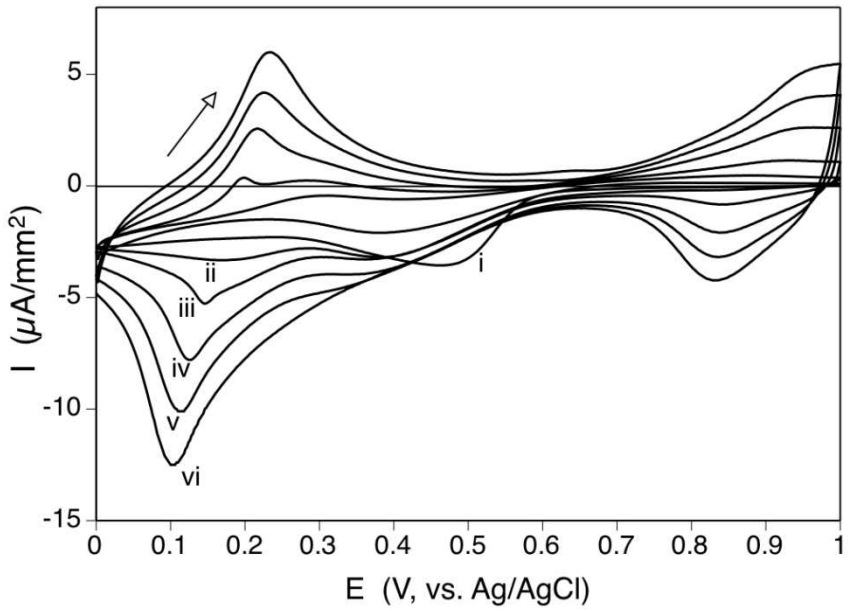

Figure S3. Growth of AuHCF layer on pAu/ITO electrode during electrodeposition process via potential cycling with scan rate, 100 mV/s in 1.0 M $KAuCl_4$, 1.0 mM $K_3Fe(CN)_6$, 0.1 M KNO_3 solution (pH 3.2); each of i to vi represents 1^{st}, 5^{th}, 10^{th}, 20^{th}, 30^{th} and 40^{th} cycle.

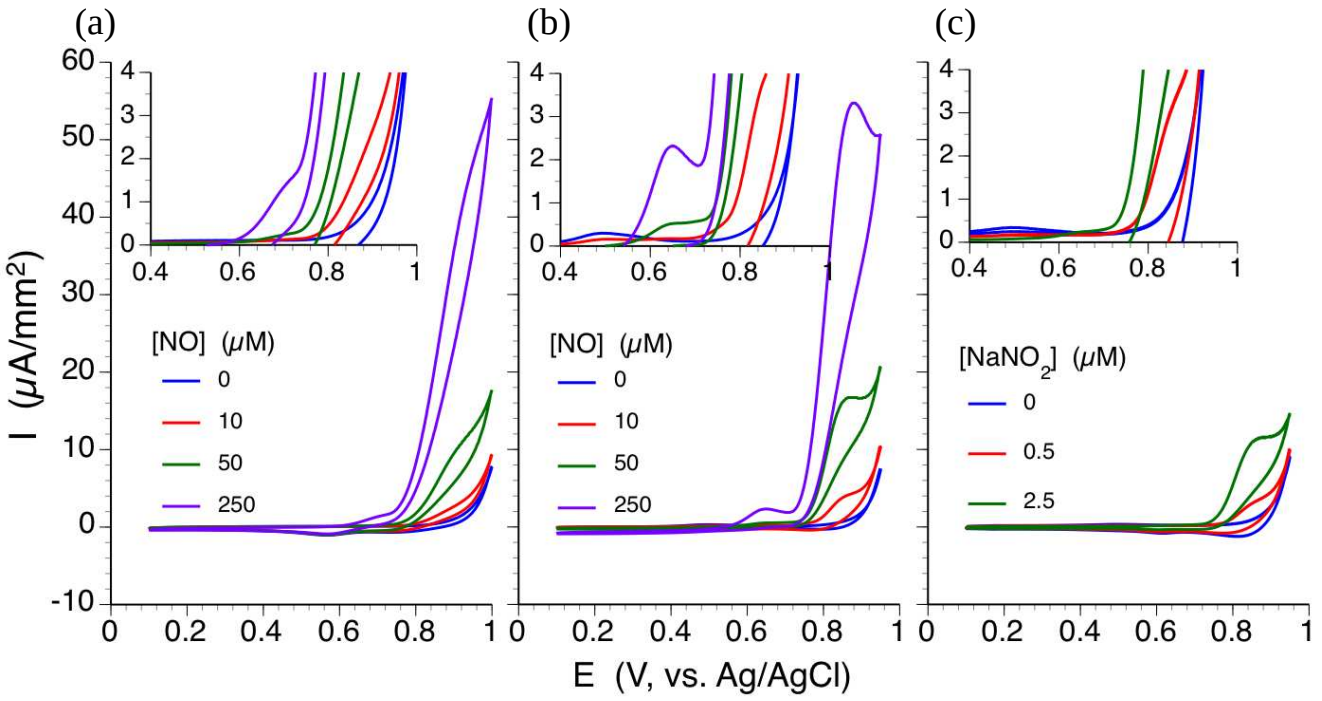

Figure S4. Cyclic voltammetry study of NO and nitrite oxidation on Au metal electrode (1 mm, d.). (a) NO oxidation on bare Au electrode; (b) NO oxidation on modified Au electrode having AuHCF layer; (c) nitrite oxidation on modified Au electrode having AuHCF, in a solution containing 0.1M KCl and 0.01M HCl at 50 mV/s scan rate. In (a) and (b) a pre-wave grows as NO concentration increases from potential around + 0.6 V (vs. Ag/AgCl), which is absent in (c). Therefore, this likely indicates adsorption and oxidation of NO on both bare Au and AuHCF electrodes to nitrite at the potential range of the pre-wave (+ 0.6 V ~ + 0.75 V). In addition, larger pre-wave current from AuHCF electrode compared to that of bare Au electrode implies enhanced catalytic activity on AuHCF surface for NO oxidation to nitrite. As a result, we applied + 0.75 V at WE when using electrodes modified with AuHCF layer for amperometric NO detection in this study.

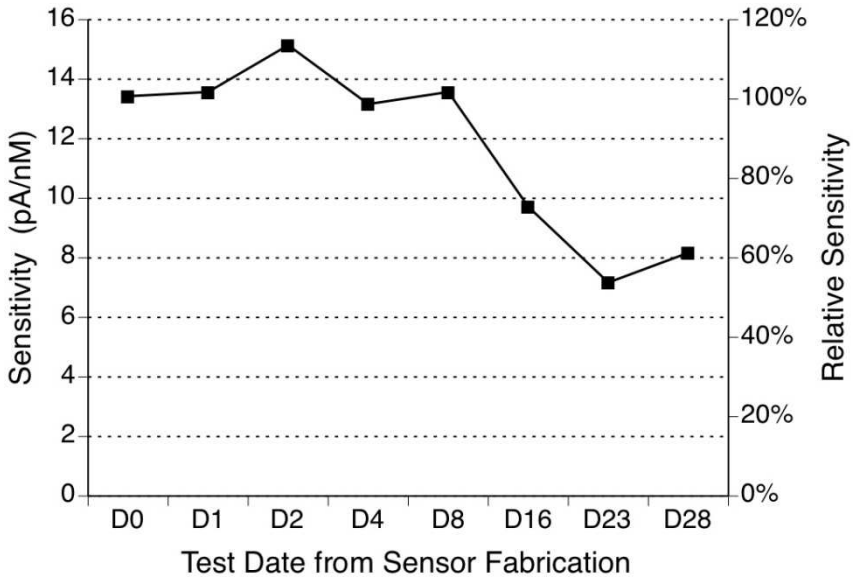

Figure S5. Sensor sensitivity change over time. Patterned electrode based NO sensor was regularly calibrated for 4 week with solutions containing different levels of NO. Slopes of calibration curves were recorded. Even after 4 week the sensitivity is still maintained at ~ 60% level of initial one. However, sensor noise levels increase over time, therefore this results in gradual increase of sensor's limit of detection (data not shown).

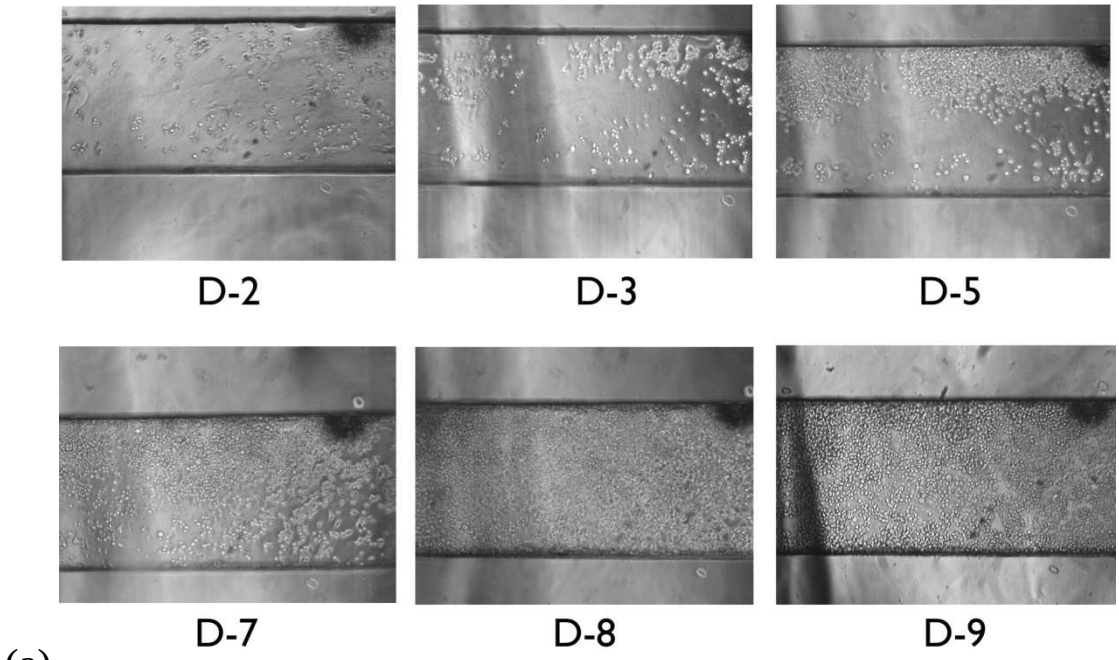

(a)

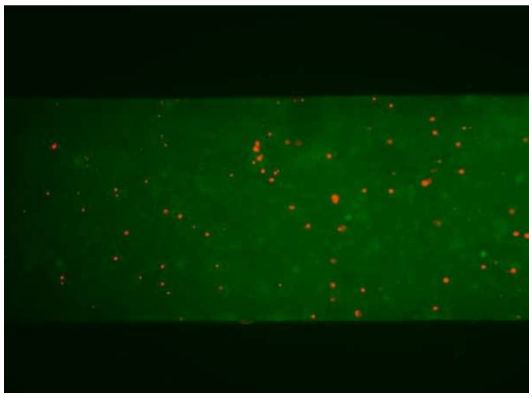

(b)

Figure S6. Cell (RAW264.7) growth on channel surface within microfluidic NO detector. Cells were attached on surface of PU film that was previously bonded to embossed PETG substrate via Ar/O_2 plasma treatment. This plasma treatment as well as fibronectin coating (see Experimental section in main text) enhance cell attachment on PU surfaces. (a) Cells form a confluent monolayer after 8 day of perfusion of DMEM containing high glucose (4.5 g/L), 15% fetal bovine serum, glutamine (1 %) and pyruvate (110 mg/L). At the end of day-8, media was change to DMEM containing LPS (1 µg/mL) and perfused for 24 h, then D-9 image was taken. (b) Composite dark field image of D-9 in (a) for cell live/death analysis. Live and dead cells emit green and red fluorescence, respectively. Therefore, most cells were found viable after the prolonged contact with LPS containing media.

Table S1. Measured amperometric selectivity coefficients of the common interfering species (see below for the detailed description for calculation).

Species, j	$NaNO_2$	NH_4Cl	Ascorbate	Glutathione
$\log(k_{NO,\,j})$	-5.9	-5.4	-5.9	-4.9

[Measurement of Amperometric Selectivity Coefficient from Experimental Results]

To quantitatively discuss the amperometric selectivity of the NO sensors examined, 'amperometric selectivity coefficient ($k_{i,j}$)' was calculated based on a methodology reported previously.[1] This method defines amperometric selectivity as described in eqs. 1 and 2 below. For any amperometric device, the total current (I_t) can be described by the linear combination of two terms proportional to the concentration (C) of the target analyte (i, i.e., NO in this study) and the interfering species (j, e.g., ascorbate or nitrite) as shown in eq. 1.

$$I_t = B\,(C_i + \sum_{j}^{n} k_{i,j}^{amp} C_j) \qquad (1)$$

Then, the constant B denotes the true amperometric sensitivity of the given sensor toward the analyte (NO). Further, the $k_{NO,j}$ can be experimentally obtained via use of the separate solution method; current levels were recorded separately for test solutions containing the analyte and the interfering species. Based on the ratio of amperometric sensitivity ($\Delta I/C$) obtained for each species, the selectivity coefficient was calculated by eq. 2.

$$k_{i,j}^{amp} = (\Delta I_j / C_j) / (\Delta I_i / C_i) \qquad (2)$$

where $\Delta I_j = I_j - I_b$ and $\Delta I_i = I_i - I_b$

I_i : the current recorded for the analyte (NO)

I_j : the current recorded for the interfering species

I_b: the basal current recorded for the blank solution

Typically, two or more sensor strips (without attachment to microfluidic devices) were tested. For an individual NO sensor, the average values of amperometric sensitivity ($\Delta I/C$) and selectivity coefficients were obtained from the multiple measurements (n > 3) for each species. For convenience, the $k_{NO,\,j}$ was subsequently transformed into logarithmic form, i.e., $\log(k_{NO,\,j})$.

1. Wang, J. *Talanta* **1994**, *41* (6), 857-863